

Techno-economic analysis of a hydrogen fuel cell hybrid system and corresponding optimum matching design for hydrogen fuel cell forklifts

Yu Li¹, Qi Wu², Tiande Mo¹, Fengxiang Chen², Yang Luo^{1,3} and Chuliang Shan¹

¹ Smart City Division, Hong Kong Productivity Council, Hong Kong, People's Republic of China


² School of Automotive Studies, Tongji University, Shanghai, People's Republic of China

³ Department of Materials, ETH Zürich, Switzerland

ABSTRACT

Conventional forklifts face serious issues, with internal combustion engine models causing indoor pollution, and lead-acid battery variants having slow charging and reduced power output as the charge diminishes. To address these drawbacks, this paper introduces a 2.5-tonne fuel cell forklift designed for Hong Kong's bustling logistics, warehousing, and transportation needs. It presents the development of dynamic simulation and cycle condition models, incorporating life cycle cost and average efficiency functions. Simulations reveal that selecting a 50-cell stack (rated at 11.8 kW) is the most cost-effective option, reducing hydrogen consumption by 2.3% using Technique for Order of Preference by Similarity to Ideal Solution (TOPSIS) optimisation. Cycle conditions do not alter the stack's optimal working voltage. However, the stack's voltage is influenced by stack and hydrogen prices, requiring an optimal design based on Hong Kong's actual costs. This study provides a theoretical foundation for future fuel cell forklift design through techno-economic analysis.

KEYWORDS Fuel cell forklift; hybrid system; life cycle cost; working voltage; Technique for Order of Preference by Similarity to Ideal Solution (TOPSIS); sensitivity analysis

CONTACT Yu Li  yli@hkpc.org

Received 6 October 2023

1. Introduction

The progressively dire state of global environmental pollution and climate change can be attributed to the extensive reliance by humanity on fossil fuels (Falcone et al., 2021). Hydrogen, functioning as a clean and versatile secondary energy source, offers a viable pathway to cost-effective decarbonisation. Recent years have witnessed a rapid and robust growth in the hydrogen economy, epitomised by advancements in hydrogen fuel cell technology (Chakraborty et al., 2022). This development signifies a global shift towards a cleaner and more sustainable energy landscape. Fuel cells represent a novel power source that enhances energy efficiency while concurrently diminishing exhaust emissions. Their inherent advantages underscore their crucial role in various modes of transportation. Presently, the primary hindrances to the widespread commercial adoption of fuel cells in the transportation sector are inadequate hydrogen refuelling infrastructure, a lack of supporting services, and technical challenges within power systems.

Forklifts are indispensable industrial handling vehicles extensively employed in warehouses, ports, and various operational settings. In a bid to curtail air pollution, traditional internal combustion engine forklifts are gradually giving way to lead-acid battery-powered forklifts. However, these lead-acid battery forklifts suffer from several shortcomings, including limited range, protracted charging times, and a reduction in operational efficiency as the battery's level of charge diminishes (Radica et al.,

2021). To address these limitations and deliver an eco-friendly solution, the introduction of hybrid fuel cell/lithium battery forklifts is emerging as an ideal choice for powering these vehicles. Such hybrid systems offer sustained high working capacity without environmental harm. Forklifts, with their distinctive characteristics such as limited operating range, lighter weight, and relatively modest technical power system requirements, are poised to lead the way in fuel cell applications. Typically confined by the constraints of storage facilities, these forklifts only require a cost-effective, small 35 MPa standard hydrogen refuelling station within the base in which they operate. Consequently, the promotion of fuel cell-powered forklifts is not tethered to the extent of hydrogen refuelling infrastructure coverage.

As far back as 2007, E Chan et al. (2007) embarked on the design of a hybrid forklift power system, integrating both fuel cells and batteries within an active hybrid configuration. Additionally, Das et al. (Das et al., 2017) developed a comprehensive model for a fuel cell hybrid forklift drive system utilising Matlab/Simulink. While this model primarily focused on a static representation of the fuel cell system, it successfully validated the power system's capability to meet the performance demands of the forklift. Moving forward, E Hosseinzadeh (Hosseinzadeh et al., 2013) et al. delved into the comparison of various combinations of fuel cells and lead-acid batteries, assessing their impact on forklift performance and hydrogen consumption. Their work revealed a crucial trade-off: a larger battery, while delaying the fuel cell's startup, resulted in reduced hydrogen consumption. However, it also added

to the vehicle's weight, necessitating a delicate balance between battery capacity and weight considerations. Evaluating the economics of fuel cells often hinges on a perspective that assumes limited-scale utilisation, resulting in differing conclusions when compared to conventional energy sources. For instance, N Metzger et al. (Metzger and Li, 2022) contended that lithium batteries exhibited a lower lifecycle cost for forklifts when compared with proton-exchange membrane fuel cells. Conversely, J Leaver et al. (Leaver and Gillingham, 2010) argued that, accounting for carbon taxes, hydrogen fuel cells prove to be more cost-effective than internal combustion engines and lithium batteries. It is crucial to note that many of these cost assessment factors in additional elements, such as infrastructure development and various economic variables, have led to the formulation of more intricate models (Renquist et al., 2012).

It is a common practice to assess the efficacy of a specific technology primarily through economic evaluations, often overlooking the optimisation of system design from a cost-centric perspective. For instance, Zheng et al. (2014) introduced an energy management strategy grounded in Pontryagin's minimum principle. Their analysis demonstrated its potential to yield cost savings and extend the system's service life. Similarly, Kumaraswamy et al. (Kumaraswamy and Quaicoe, 2017) explored the impact of operating parameters on operational expenses, though primarily focusing on maximum power and maximum efficiency. In contrast, some research endeavours have delved into the influence of system design choices on costs, particularly in the realm of solid oxide fuel cell/gas turbine hybrid power generation. Cheddie (Cheddie and Murray, 2010) et al., for instance, investigated the cost implications of varying cell voltage. It is worth noting that these thermo-economic assessments encompassed not only fuel cell power generation but also the integration of gas turbines for waste heat recovery, providing a more holistic view of the cost dynamics.

In the context outlined above, this paper presents a comprehensive study of a 2.5-tonne hybrid forklift, combining fuel cell and lithium battery technologies, situated in Hong Kong. Detailed models for the corresponding power system and operational conditions were established. Leveraging these dynamic models, functions were developed for evaluating the forklift's life cycle cost and average efficiency. Subsequently, simulations were conducted based on these models to determine the optimal power settings and working voltage for the forklift's fuel cell stack. To further enhance hydrogen utilisation efficiency, the Technique for Order of Preference by Similarity to the Ideal Solution (TOPSIS) methodology was applied. Finally, a sensitivity analysis was carried out, considering variables such as cycle conditions, stack performance, stack design life, service time, stack pricing, and hydrogen pricing. This analysis provides a solid theoretical foundation for informing the future design and deployment of fuel cell-powered forklifts.

2. Fuel cell forklift power system modelling

2.1. Fuel cell forklift configuration

Given the bustling logistics and warehousing in Hong Kong, this paper introduces a 2.5-tonne counterbalanced forklift featuring a hybrid power system consisting of a 10 kW proton-exchange membrane fuel cell and an 80 V/125 Ah lithium-ion battery, as illustrated in Figure 2. Table 1 provides a summary of its specific parameters.

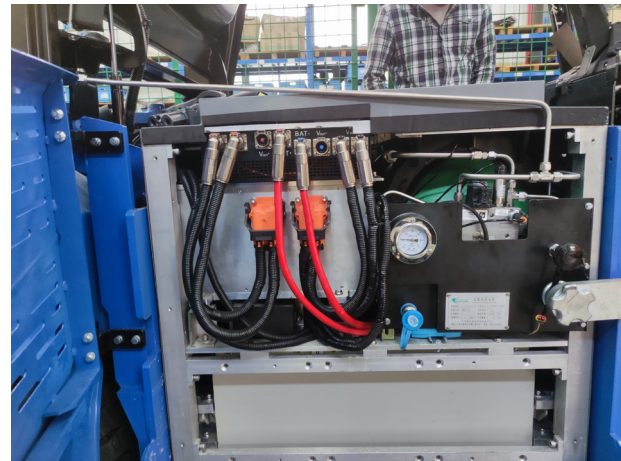


Figure 1. Photograph of the forklift.

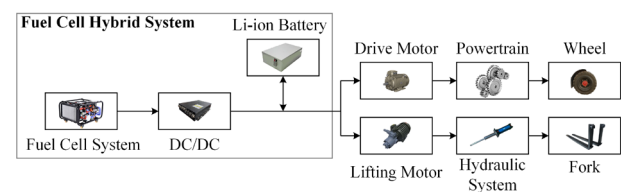


Figure 2. Forklift power system architecture.

Table 1. Forklift and stack parameters.

Self-weight (kg)	Rated load capacity (kg)	Maximum full load driving speed (km/h)	Rated full load lifting speed (mm/s)	Rated full load lowering speed (mm/s)
4285	2500	13	280	430
Number of stack cells (pieces)	Active area size (cm ²)	Rated power (kW)	Rated current (A)	Rated individual voltage (V)
52	285	12.27	370.5	0.637

2.2. Forklift and fuel cell system dynamics modelling

In the longitudinal force analysis of the forklift, due to the low speed of the forklift and negligible air resistance, the forklift moves at a speed of v (Genta, 1997).

$$v = \int \frac{F_t - F_f - F_i - F_b}{\delta m} dt, \tag{1}$$

where F_i is the driving force, F_f is the rolling resistance, F_g is the gradient resistance, F_a is the acceleration resistance, F_b is the braking force, δ is the conversion coefficient of the rotating mass, and m is the total mass of the forklift.

The forklift lifting system can be approximately calculated based on the principle of conservation of energy. The operating voltage of a proton exchange membrane fuel cell can be corrected by activation loss, ohmic loss, and mass transfer loss based on the Nernst equation, and then its single cell voltage is (O'hayre et al., 2016):

$$U_{\text{cell}} = 1.195 + \frac{RT}{2F} \ln(P_{\text{H}_2} P_{\text{O}_2}^{\frac{1}{2}}) - \frac{RT}{2\alpha F} \ln\left(\frac{I_{\text{st}} c_{\text{O}_2}^0}{I_0^0 c_{\text{O}_2}^{\text{cl}}}\right) - \frac{I_{\text{st}} \delta_{\text{mem}}}{A_{\text{st}} \sigma_{\text{mem}}}, \quad (2)$$

where R is the ideal gas constant, T is the stack temperature, F is the Faraday constant, P_{H_2} is the hydrogen partial pressure, P_{O_2} is the oxygen partial pressure, α is the transport coefficient, $c_{\text{O}_2}^0$ is the reference oxygen concentration, $c_{\text{O}_2}^{\text{cl}}$ is the catalytic layer oxygen concentration, I_{st} is the stack current, I_0^0 is the stack current at the reference concentration, A_{st} is the active area size, δ_{mem} is the proton exchange membrane thickness, and σ_{mem} is the proton exchange membrane conductivity.

Modelling the anode and cathode flow channels, gas diffusion layer, and proton exchange membrane allowed us to derive the parameters for calculating the dynamic stack voltage. The resulting fuel cell polarisation curves are displayed in Figure 3. These curves demonstrate relative errors within $\pm 1\%$ when compared to the experimental data from the manufacturer's stack test, affirming the accuracy of the stack model.

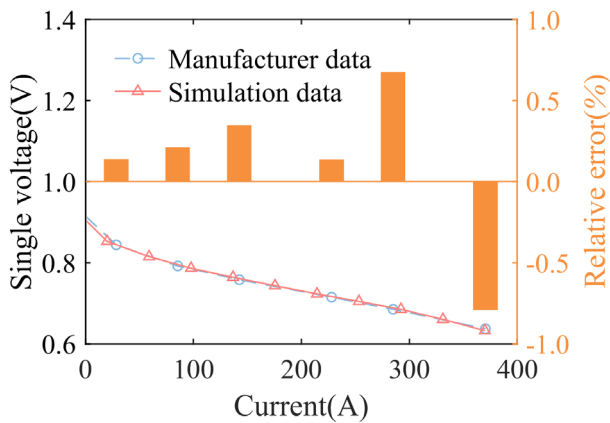


Figure 3. Stack polarisation curve.

Based on the stack model, the entire fuel cell system model can be obtained by adding balance of plant (BOP) models such as the hydrogen/air supply system and thermal management system. For the fuel cell system, the BOP efficiency η_{BOP} is obtained by Equation (3).

$$\eta_{\text{BOP}} = \frac{I_{\text{st}} U_{\text{st}} - P_{\text{BOP}}}{I_{\text{st}} U_{\text{st}}}, \quad (3)$$

where U_{st} is the fuel cell stack voltage, and P_{BOP} is the power of BOP such as the blower, water pump, etc.

2.3. Cycle condition modelling

The People's Republic of China Machinery Industry Standard (JB/T 3300-2010) for energy consumption testing of internal combustion forklifts (Zhang et al., 2021) was modified to align with the real working conditions of fuel cell forklifts. This ensures that the forklift operates within a 60 second cycle, equally split between loaded and unloaded conditions. By incorporating the forklift model into the cycle condition model for dynamic simulation (Figure 4), the forklift's average power was determined to be 6,103 W, with its total hydrogen consumption being 348.6 g/h, matching the real test results.

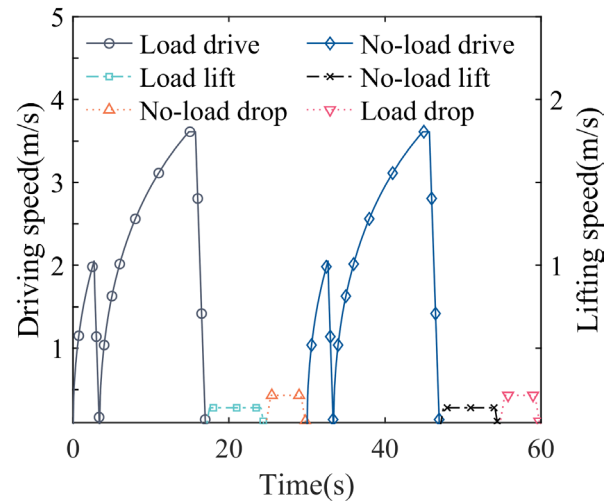


Figure 4. Forklift and fork movement.

3. Life cycle cost function, stack average efficiency function and parameter optimisation

Before deriving the relevant function, the following reasonable assumptions were made: the sole focus is the fuel cell system itself, with consideration of a single forklift rather than a fleet, whilst accounting for cash outlay without involving borrowing, and excluding policy incentives. A residual system value of 0 is assumed, and the stack's power varies solely through changes in the number of cells, with its current density polarisation curve remaining constant.

3.1. Life cycle cost function

The life cycle cost (LCC) function refers to the costs associated with a product that arise during its effective use (Wang et al., 2022). For the fuel cell system selected for the forklift truck, LCC was established as:

$$LCC = C_{st} + C_{BOP} + \int_0^T C_{op} dt + \int_0^T C_{fuel} dt, \quad (4)$$

where C_{st} is the stack cost, C_{BOP} is the BOP cost, C_{op} is the operating cost, C_{fuel} is the hydrogen cost, and T is the runtime.

For the stack cost C_{st} , based on the reference stack power P_{StDesg} of the forklift, the amplification factor $f(V_{work}, V_{design})$, which is determined by the fuel cell model in Equation (2), is used to convert its power for different working voltages, so the following is obtained:

$$C_{st} = C_1 \frac{P_{StDesg}}{f(V_{desg}, V_{work})} = C_1 \frac{n_{cell} A V_{desg} \rho}{f(V_{desg}, V_{work})}, \quad (5)$$

where C_1 is the stack unit price in HK\$/kW, n_{cell} is the number of fuel cell pieces, A is the single cell active area size in cm^2 , V_{desg} is the reference design working voltage in V, ρ is the current density in A/cm^2 , and V_{work} is the actual working voltage in V.

For the BOP cost C_{BOP} which can be considered constant when the working capacity of the system remains the same, it can be obtained as:

$$C_{BOP} = k_1 C_1 P_{StDesg}, \quad (6)$$

where k_1 is the BOP cost factor.

For the operating cost C_{op} , from a long-timescale perspective, it can be as time-dependent as the hydrogen cost, and therefore can be converted to the hydrogen cost as follows:

$$C_{op} = k_2 C_{fuel}, \quad (7)$$

where k_2 is the operating cost factor.

Taking into account the BOP efficiency calculated by the fuel cell model in Equation (3), the hydrogen cost C_{fuel} can be obtained as:

$$C_{fuel} = C_2 \int_0^T \frac{V_{heat} P_{cy}(t) M_{H2}}{LHV_{H2} V_{real}(t) \eta_{purge} \eta_{BOP}(P_{cy})} dt, \quad (8)$$

where C_2 is the hydrogen unit price in HK\$/kg, V_{heat} is the reversible voltage in V, P_{cy} is the cycle condition average working power in kW, M_{H2} is the hydrogen molecular weight in kg/mol, LHV_{H2} is the hydrogen lower heating value in kJ/mol, V_{real} is the working voltage in V, η_{purge} is the hydrogen utilisation rate which can be considered as a constant value and $\eta_{BOP}(P_{cy})$ is the BOP efficiency which is influenced by the cycle condition.

$V_{real}(t)$ is affected by the operating time of the stack, and its single-cell voltage decline can be regarded as a linear degradation of 10% for the 10,000 hours of the design life of the stack in this paper, as shown in Figure 5 (Chen et al., 2015).

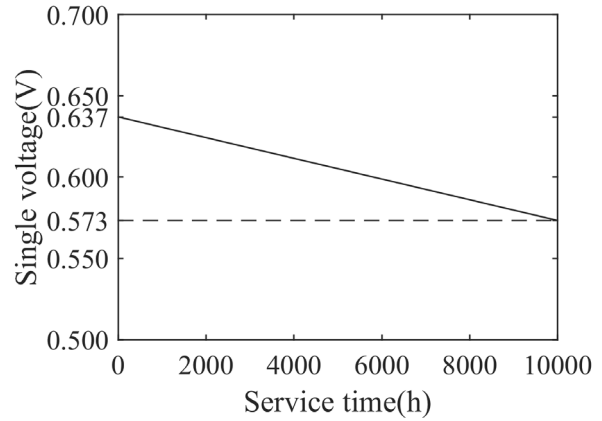


Figure 5. Stack degradation.

Substituting the above Equation (5) - (8) into Equation (4), the LCC function can be obtained as:

$$LCC = C_1 \frac{n_{cell} A V_{desg} \rho}{f(V_{desg}, V_{work})} + k_1 C_1 P_{StDesg} + (1+k_2) C_2 \int_0^T \frac{V_{heat} P_{cy}(t) M_{H2}}{LHV_{H2} V_{real}(t) \eta_{purge} \eta_{BOP}(P_{cy})} dt. \quad (9)$$

3.2. Stack average efficiency function

The probability density function $p(P_{cycle})$ of the operating power of the fuel cell system obtained from the fuel cell forklift dynamic model and the cycle condition model is shown in the following Figure 6.

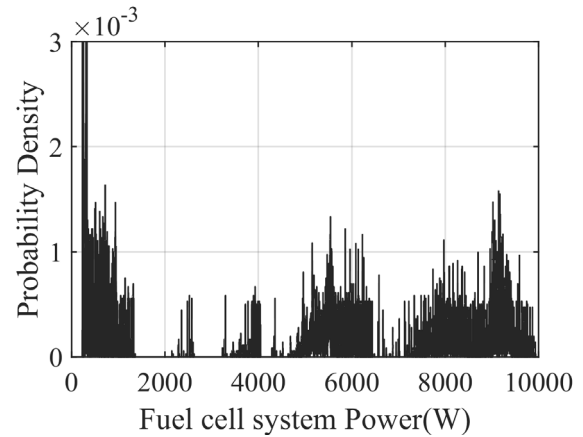


Figure 6. Working power probability density function.

Substituting this into the system, a probability density function $p(e_{st})$ of the stack efficiency can be established, and therefore, the stack average efficiency e_{st_avg} is:

$$e_{st_avg} = \int e_{st} p(e_{st}) de_{st}, \quad (10)$$

where e_{st} is the stack current efficiency.

3.3. Simulation results

The fuel cell system parameters are aligned with current technology and guided by cycle conditions. Given that the hydrogen economy in Hong Kong is still in its infancy and lacks essential infrastructure like hydrogen refuelling stations, benchmark prices are provided in Table 2, with simulation results depicted in Figure 7. Notably, lower fuel cell efficiency leads to increased hydrogen consumption throughout the lifecycle, resulting in a higher LCC. To enhance fuel cell efficiency, opting for a larger fuel cell system is necessary, albeit at a higher LCC. Thus, considering current stack and hydrogen prices in Hong Kong, selecting a 50-cell stack (rated power of 11.8 kW) for the 2.5-tonne forklift is the most suitable choice. This configuration maintains an average working voltage of 0.737 V, an average stack efficiency of 59.88%, and a notably low LCC of HK\$346,556.

Table 2. Benchmark price.

k_1	k_2	C_1	C_2
0.4	0.005	3500	80

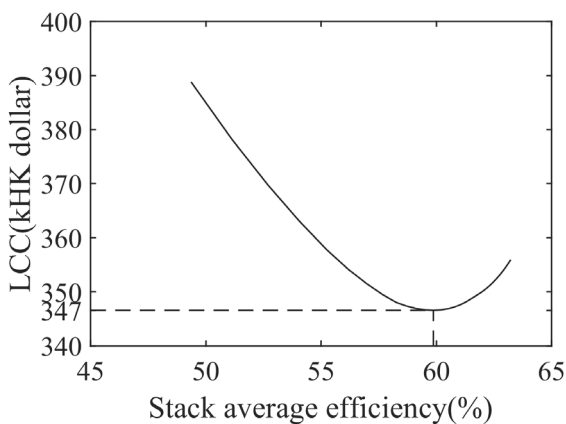


Figure 7. Baseline simulation results.

In terms of the lifecycle perspective, only 16% of the total cost is attributed to the fuel cell system, with the majority linked to hydrogen consumption. Thus, the accuracy of the LCC assessment relies on the dynamic forklift model established earlier. The current forklift incorporates a 52-cell stack, resulting in an LCC of HK\$346,634, aligning closely with the simulation optimisation outcomes, making it suitable for the current Hong Kong region. However, this forklift was originally designed with a focus on a 20 kW peak power and 6 kW average power. To fulfil this power demand, a 10 kW fuel cell system was adopted for average power, complemented by a 10 kWh (1C) lithium-ion battery to address peak power needs. This study thus lays a theoretical foundation for forklift design, emphasising lifecycle techno-economics.

3.4. TOPSIS optimisation

Given that coal serves as the primary source of hydrogen production in Hong Kong, a marginal increase in LCC is tolerable in the interest of environmental protection. Therefore, the Technique for Order of Preference by Similarity to the Ideal Solution (TOPSIS) is employed to comprehensively assess LCC and stack average efficiency. TOPSIS operates on the principle that the chosen alternative should minimise its geometric distance from the positive ideal solution while maximising its distance from the negative ideal solution, as depicted in Figure 8. This approach ensures more comprehensive utilisation of original data and minimises information loss (Yoon and Kim, 2017). As illustrated in Figure 9, the positive ideal solution (A) represents the lowest LCC and stack efficiency, though it may not be attainable, whereas the negative ideal solution (B) signifies the highest LCC and stack efficiency. The optimal solution aims to closely approach point A while distancing itself from point B within the rectangular region formed by these points. Applying TOPSIS, point P is selected with a working voltage of 0.754 V. The lowest LCC point (C) involves a total hydrogen consumption of 3,539 kg and an LCC of HK\$348,115. In contrast, optimisation point P achieves a 2.3% reduction in hydrogen consumption, totalling 3,623 kg, and a slight 0.45% increase in LCC, reaching HK\$346,556. This modest cost increase results in reduced hydrogen consumption, directly leading to a 1,848 kg reduction in CO₂ emissions per forklift.

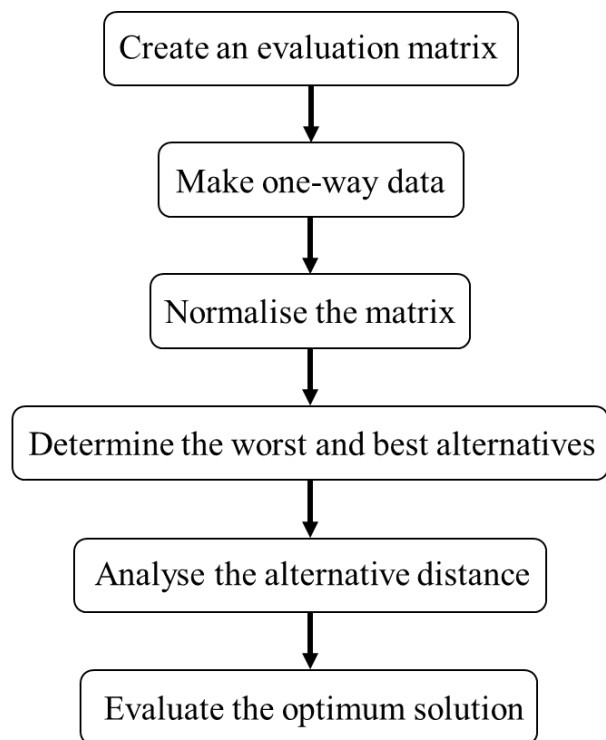


Figure 8. TOPSIS optimisation.

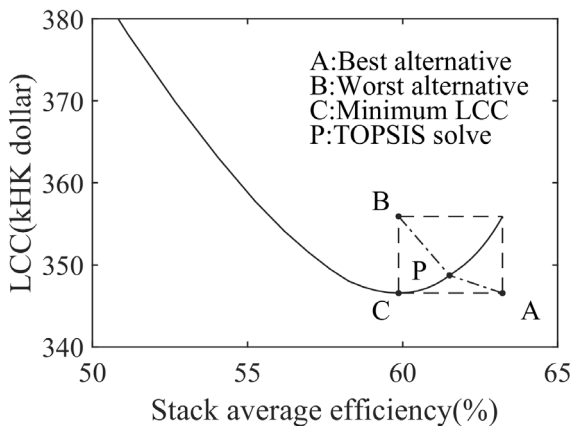


Figure 9. Topsis analysis.

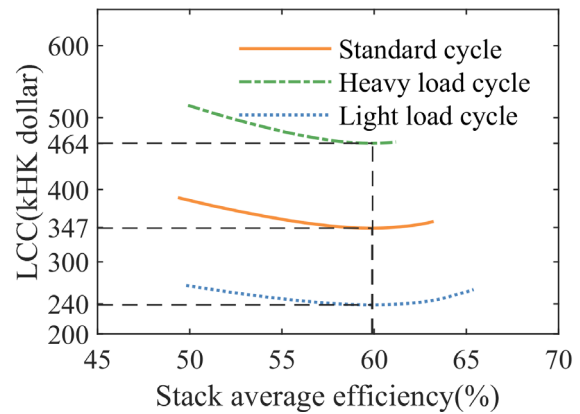


Figure 10. Effect of cycle condition on the system.

4. Sensitivity analysis

Using the aforementioned results as a baseline, sensitivity analyses were conducted in relation to factors including cycle conditions, stack performance, stack design life and service time, stack price, and hydrogen price. This enabled the anticipation of the influence of the hydrogen economy's evolution on the future design and LCC of the forklift.

4.1. Cycle condition

The forklift's average power varies across different scenarios, and corrections were made to the cycle conditions described in Section 2.4 to align with real-world work patterns. For the heavy load cycle, the unloaded condition was removed, while the light load cycle now includes a 30 second idle period in each cycle. The results, as shown in Figure 10, demonstrate that operating at different intensities does not impact the design's optimal operating voltage for the stack, which remains at 0.737 V. Consequently, for the light load cycle, an 8.0 kW rated power stack is chosen, with an 11.8 kW stack for the standard cycle and a 16.0 kW fuel cell for the heavy load cycle. The ratio between system cost and hydrogen cost in Equation (9) remains constant as the cycle conditions change; thus, the operating voltage remains unaffected. However, different cycle conditions significantly influence hydrogen consumption, thereby significantly affecting LCC.

4.2. Stack performance

Improvements in proton exchange membranes, highly active catalysts, and flow channel designs significantly enhance stack performance. Europe anticipates stack power density to reach 1.2 W/cm² @0.675V by 2030 (Urban Europe, 2019), up from 1 W/cm² @0.650V in 2020. Assuming a boost in stack power density from 0.8 W/cm² to 1.2 W/cm², albeit with no change in unit price due to increased manufacturing costs, the sensitivity analysis in Figure 11 indicates that LCC can be reduced by 3.1% and 5.5% as fuel cell performance climbs from 0.8 W/cm² to 1.0 W/cm² and 1.2 W/cm², respectively. Improved stack performance allows operation at higher efficiency voltages, selecting stacks with ratings of 11.8 kW, 12.2 kW, and 13.1 kW, respectively. Stacks with different power densities but the same rated power exhibit higher single voltages when operating at the same power, thereby enhancing efficiency, reducing hydrogen consumption, and lowering LCC. A slight increase in stack power particularly benefits efficiency, motivating the use of higher-voltage operation.

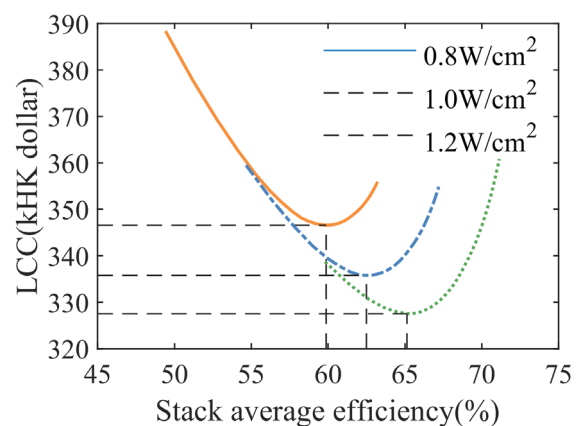


Figure 11. Effect of stack performance on the system.

4.3. Stack design life and service time

European institutions estimate that stack design life will be prolonged from 15,000 hours in 2020 to 30,000 hours in 2030 (Urban Europe, 2019). When considering the lifetime of the stack, levelised life cycle cost (LLCC) is introduced to assess the average cost per hour of the forklift:

$$LLCC = \frac{LCC}{t} \quad (11)$$

Using the benchmark as an example, Figure 12 illustrates how LLCC changes with increasing stack service time. As service time grows, the stack's LLCC decreases rapidly, while operating and hydrogen LLCC gradually rise due to stack and system degradation. Consequently, total LLCC initially decreases and then increases with service time. In this benchmark, the optimal service time is 17,800 hours, resulting in the lowest LLCC of HK\$34.66 per hour, though the difference diminishes later. Table 3 below presents the simulation results, revealing that a longer stack design life favours selecting a larger stack for higher efficiency and reduced hydrogen LLCC, resulting in declining total LLCC. Extending the system service time also reduces LLCC unless it leads to increased operating costs. It is worth noting that a longer stack design life affects BOP cost factors and shortens the optimal service time.

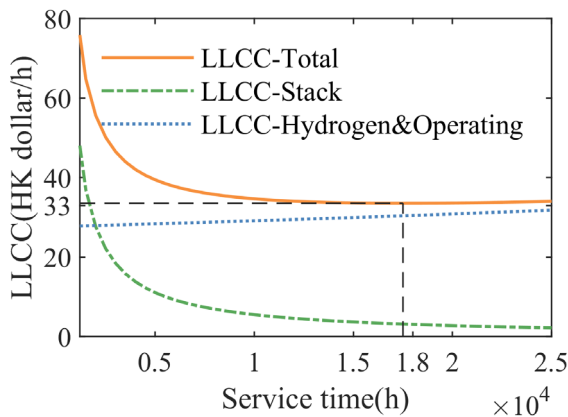


Figure 12. Variation of LLCC with service time.

Table 3. Effect of stack design life and service time on the system.

Design life (h)	Minimum LLLC (HK\$/h)	Number of stack cells (pieces)	Working voltage (V)	Stack efficiency (%)	Optimal service time (h)	LLC under optimal service time (HK\$/h)
10000	34.66	50	0.737	59.88	17800	33.55
20000	31.55	72	0.770	62.57	30000	31.11
25000	30.79	80	0.778	63.22	35000	30.49

4.4. Stack price

As the fuel cell market expands, stack prices are expected to decrease. The US DOE estimates that current fuel cell system prices range from US\$180-230/kW, with mass production costs of around US\$50/kW, and an ultimate target of US\$30-45/kW (Miller et al., 2020). European institutions predict stack prices to be less than 50 €/kW by 2030 (Urban Europe, 2019). In China, fuel cell system prices are projected to drop to ¥3500, ¥1000, and ¥500/kW by 2025, 2035, and 2050, respectively (Zhang, 2021). Conducting sensitivity analysis on fuel cell prices with other parameters held constant, the results in Figure 13 show that as system prices decrease to 2500, 1500, and 350 HK\$/kW, the corresponding stack rated powers are 13.7 kW, 17.9 kW, and 41.1 kW, respectively. Consequently, LCC decreases significantly by 3.65%, 8.21%, and 16.93%. When system prices drop to 1/10 of the current price, power increases by approximately 3.5 times. A larger stack allows for operation at a higher-efficiency voltage, saving hydrogen without additional cost if system prices decrease.

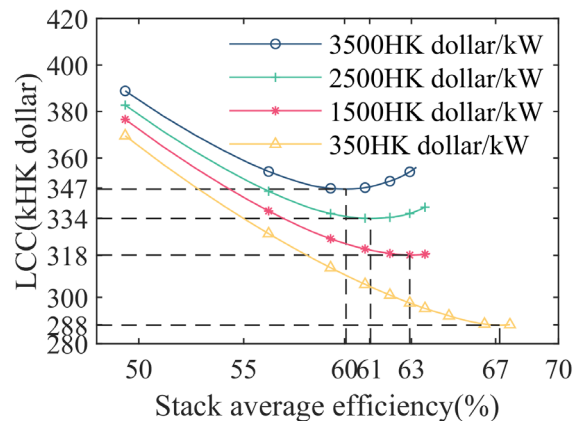


Figure 13. Impact of stack price on the system.

4.5. Hydrogen price

Regarding hydrogen prices, the US DOE estimates that current consumer prices are in the range of \$13-16/gge but could decrease to \$5-10/gge for large-scale applications, with an ultimate target of less than \$4/gge (Miller et al., 2020). China aims to achieve prices of

¥40/kg by 2025, ¥30/kg by 2035, and ¥20/kg by 2050 (Ren et al., 2020). The simulation utilises Hong Kong's current hydrogen price as a benchmark, revealing that decreasing hydrogen prices significantly reduces LCC. For instance, under a stack price of HK\$3500/kW, a hydrogen price decrease of HK\$80/kg to HK\$15/kg results in a 71% LCC reduction. When the stack price drops to HK\$350/kW, a decrease in hydrogen prices leads to a 75% LCC reduction. Analysing the stack's working voltage shows that as hydrogen prices decrease, the system can operate at lower voltages, thereby reducing stack costs and LCC. The choice of working voltage should align with the cost of the fuel cell system and hydrogen in Hong Kong.

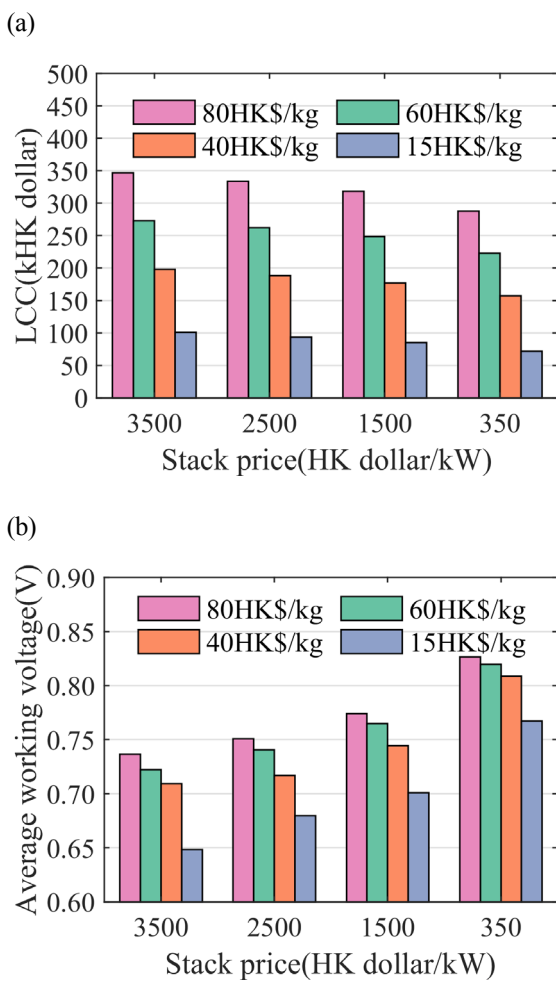


Figure 14. Impact of hydrogen price on the system: (a) impact on the LCC; and (b) impact on the average working voltage.

5. Conclusion

This paper introduces a hybrid fuel cell/lithium battery forklift in Hong Kong and establishes corresponding models for the fuel cell power system and cycle conditions.

Using these models, techno-economic analysis was conducted, offering a theoretical foundation for future fuel cell forklift designs. The key conclusions are as follows:

- (1) It is recommended to use a 50-cell stack (11.8 kW) under current conditions, yielding an average working voltage of 0.737 V, an average stack efficiency of 59.88%, and an LCC of HK\$346,556.
- (2) Optimising the working voltage to 0.754 V through TOPSIS increases LCC by 0.45%, but reduces hydrogen consumption by 2.3% and CO₂ emissions by 1,848 kg per forklift.
- (3) Cycle conditions affect LCC but have limited impact on the optimal design voltage.
- (4) Improved stack performance allows for fewer cells but increased power. Higher stack power density with a higher working voltage reduces LCC.
- (5) A longer stack design life supports the use of a larger stack for efficiency gains and reduces the levelised life cycle cost (LLCC). Extending the system service time also lowers LLCC.
- (6) A 10-fold reduction in stack price allows for a roughly 3.5 fold increase in stack power.
- (7) Decreasing hydrogen prices significantly reduces LCC, with the sensitivity to hydrogen price increasing as stack prices decrease. The optimal design should consider the actual system and hydrogen costs in Hong Kong.

Acknowledgments

The work was funded by the Innovation and Technology Fund (ITF) of the Government of Hong Kong SAR under Grant No. PRP/067/19AI and the project supported by State Key Laboratory of Powder Metallurgy, Central South University, Changsha, China.

Notes on contributors



Mr Yu Li is the Associate Principle Consultant at Hong Kong Productivity Council (HKPC). He received his MSc in Energy and Environment from City University of Hong Kong, and MBA from Hong Kong University of Science and Technology. He has strong track records as project manager or project consultant in a number of Hong Kong Innovation and Technology Fund (ITF) R&D projects. His current research is mainly focused on hydrogen technologies, electric vehicles, battery systems, and smart systems.



Mr Qi Wu is a master's student in vehicle engineering at Tongji University. He received his Bachelor of Engineering degree from Jilin University. He has professional knowledge in the integration, matching, and optimisation control technology of PEMFC hybrid power systems.



Dr Tiande Mo is the Head of the Green and Smart Mobility in the Hong Kong Productivity Council (HKPC). He has 20 years of working experience in both academia and industry and has managed more than 20 mega-sized R&D projects funded by Hong Kong Innovation and Technology, including electric vehicles, hydrogen vehicles, chargers, battery systems, smart on-board systems and autonomous driving technologies. He is the Vice Chairman of Connected Vehicles of the Society of Automotive Engineers, Hong Kong Section (SAE-HK). He is also a Professional Member of the Association for Computing Machinery (ACM).



Prof Fengxiang Chen is an Associate Professor and Ph.D. supervisor at the College of Automotive Studies at Tongji University. He received his Ph.D. degree in Engineering from the Department of Automation at Shanghai Jiao Tong University. His research primarily focuses on the integration, control and modelling of fuel cell systems. He has led two national-level research projects and two projects at the provincial and ministerial levels. He has published a total of 61 academic papers, including 20 SCI papers. Additionally, he holds 11 invention patents.



Dr Yang Luo received his double Ph.D. degrees in Chemical Technology from the Institute of Process Engineering, Chinese Academy of Sciences and in Applied Physics from the City University of Hong Kong (2020). He is currently a Researcher at the Hong Kong Productivity Council (HKPC)/City University of Hong Kong. He is particularly interested in researching environmental and energy materials, green hydrogen technologies, and wearable electronics. He has completed previous postdoctoral and early-career research at The University of Hong Kong, Swiss Federal Laboratories for Materials Science and Technology (EMPA), and ETH Zurich.



Mr Chuling Shan is the consultant of the Hong Kong Productivity Council. He obtained his Bachelor's Degree in Automotive Engineering in 2013. After that, he obtained a Master's Degree in Automotive Engineering Design from The Hong Kong Polytechnic University. He has more than 9 years of R&D working experience in automotive system development, such as autonomous driving systems, autonomous vehicles, hydrogen fuel cell systems, EV chargers, and IoT systems, etc.

References

- [1] Chakraborty S, Dash SK, Elavarasan RM, Kaur A, Elangovan D, Meraj ST, Kasinathan P and Said Z (2022). Hydrogen Energy as Future of Sustainable Mobility. *Frontiers in Energy Research*, 10.
- [2] Chan E, Dawson F, Bekker H and Livshits E (2007). *A Software Simulation Program for a Hybrid Fuel Cell –Battery Power Supply for an Electric Fork Lift*. In: European Conference on Power Electronics and Applications. Aalborg: IEEE, pp. 1-10.
- [3] Cheddie DF and Murray R (2010). Thermo-economic modeling of a solid oxide fuel cell/gas turbine power plant with semi-direct coupling and anode recycling. *International Journal of Hydrogen Energy*, 35(20), pp. 11208-11215.
- [4] Chen H, Pei P and Song M (2015). Lifetime prediction and the economic lifetime of Proton Exchange Membrane fuel cells. *Applied Energy*, 142, pp. 154-163.
- [5] Das HS, Tan CW and Yatim AHM (2017). Fuel cell hybrid electric vehicles: A review on power conditioning units and topologies. *Renewable and Sustainable Energy Reviews*, 76, pp. 268-291.
- [6] Falcone PM, Hiete M and Sapio A (2021). Hydrogen economy and sustainable development goals: Review and policy insights. *Current Opinion in Green and Sustainable Chemistry*, 31, pp. 100506.
- [7] Genta G (1997). *Motor vehicle dynamics: modeling and simulation*. World scientific.
- [8] Hosseinzadeh E, Rokni M, Advani SG and Prasad AK (2013). Performance simulation and analysis of a fuel cell/battery hybrid forklift truck. *International Journal of Hydrogen Energy*, 38(11), pp. 4241-4249.
- [9] Kumaraswamy KV and Quaicoe JE (2017). Standalone fuel cell generation system with different tracking techniques: economic analysis. *IET Renewable Power Generation*, 11(9), pp. 1186-1193.
- [10] Leaver J and Gillingham K (2010). Economic impact of the integration of alternative vehicle technologies into the New Zealand vehicle fleet. *Journal of Cleaner Production*, 18(9), pp. 908-916.

- [11] Metzger N and Li X (2022). Technical and Economic Analysis of Fuel Cells for Forklift Applications. *ACS Omega*, 7(22), pp. 18267-18275.
- [12] Miller EL, Thompson ST, Randolph K, Hulvey Z, Rustagi N and Satyapal S (2020). US Department of Energy hydrogen and fuel cell technologies perspectives. *MRS Bulletin*, 45(1), pp. 57-64.
- [13] O'hayre R, Cha SW, Colella W and Prinz FB (2016). *Fuel cell fundamentals*. John Wiley & Sons.
- [14] Radica G, Tolj I, Markota D, Lototskyy MV, Pasupathi S and Yartys V (2021). Control strategy of a fuel-cell power module for electric forklift. *International Journal of Hydrogen Energy*, 46(72), pp. 35938-35948.
- [15] Renquist JV, Dickman B and Bradley TH (2012). Economic comparison of fuel cell powered forklifts to battery powered forklifts. *International Journal of Hydrogen Energy*, 37(17), pp. 12054-12059.
- [16] Ren X, Dong L, Xu D and Hu B (2020). Challenges towards hydrogen economy in China', *International Journal of Hydrogen Energy*. 45(59), pp. 34326-34345.
- [17] Tingyan W, Qingdan H, Chongzhi Z, Huihong H and Haoyong S (2022). Economic Operation Strategy of Multitype Emergency Power Supply Taking into Account Carbon Cost. *International Energy Journal*, 22(4).
- [18] Urban Europe (2019). Strategic research and innovation agenda 2.0. *JPI Urban Europe*, Vienna.
- [19] Yoon KP and Kim WK (2017). The behavioral TOPSIS. *Expert Systems with Applications*, 89, pp. 266-272.
- [20] Zhang E, Zhuo J, Hou L, Fu C and Guo T (2021). Comprehensive annoyance modeling of forklift sound quality based on rank score comparison and multi-fuzzy analytic hierarchy process. *Applied Acoustics*, 173, pp. 107705.
- [21] Zhang X (2021). The Development Trend of and Suggestions for China's Hydrogen Energy Industry. *Engineering*, 7(6), pp. 719-721.
- [22] Zheng CH, Xu GQ, Park YI, Lim WS and Cha SW (2014). Prolonging fuel cell stack lifetime based on Pontryagin's Minimum Principle in fuel cell hybrid vehicles and its economic influence evaluation. *Journal of Power Sources*, 248, pp. 533-544.